Nitroxyl Model Complexes

International Edition: DOI: 10.1002/anie.201605026
German Edition: DOI: 10.1002/ange.201605026

Redox Non-Innocence of Nitrosobenzene at Nickel

Subrata Kundu, S. Chantal E. Stieber,* Maryline G. Ferrier, Stosh A. Kozimor, Jeffery A. Bertke, and Timothy H. Warren**

Abstract: *Nitrosobenzene (PhNO) serves as a stable analogue of nitroxyl (HNO), a biologically relevant, redox-active nitric oxide derivative. Capture of nitrosobenzene at the electron-deficient β-diketiminato nickel(I) complex [$^{i}Pr_2NN_{F6}$]Ni results in reduction of the PhNO ligand to a $(PhNO)^{\bullet-}$ species coordinated to a square planar Ni^{II} center in [$^{i}Pr_2NN_{F6}$]Ni(η^2-ONPh). Ligand centered reduction leads to the $(PhNO)^{2-}$ moiety bound to Ni^{II} supported by XAS studies. Systematic investigation of structure–reactivity patterns of $(PhNO)^{\bullet-}$ and $(PhNO)^{2-}$ ligands reveals parallels with superoxo $(O_2)^{\bullet-}$ and peroxo $(O_2)^{2-}$ ligands, respectively, and forecasts reactivity patterns of the more transient HNO ligand.*

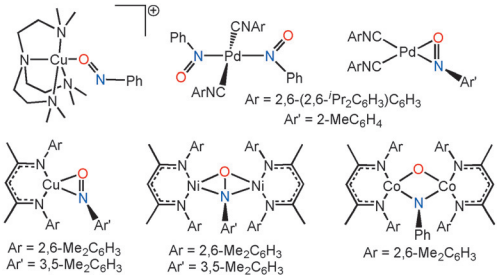

Figure 1. Representative examples of *C*-nitroso complexes.

The coordination chemistry of redox non-innocent *C*-nitroso (RNO) ligands is of paramount importance owing to their biological relevance and diverse reactivity patterns.[1,2] Moreover, PhNO and PhNHOH may serve as stable analogues of relatively reactive nitroxyl (HNO) and hydroxylamine (NH_2OH) ligands, respectively, thought to be endogenously produced and involved in various biotransformations connected to nitric oxide.[3] Notably, HNO can substitute for isoelectronic O_2 in the manganese containing quercetin dioxygenase and exhibits nitroxygenase activity.[4] Along with the biological importance of nitrosoarenes, Ni and Cu activated *C*-nitroso compounds have also been shown to participate in nitrene transfer and allylic C–H amination reactions, respectively.[5]

Nitrosobenzene has also been used as a surrogate for O_2 in copper chemistry, resulting in the κ^1-O nitrosobenzyl radical bound to a tripodal copper complex in $LCu^{II}(\kappa^1\text{-O-ONPh})^{\bullet-}$ (L = tris-(2-dimethylaminoethyl amine) (Figure 1) related to end-on superoxo complexes $[Cu^{II}]\text{-}O_2$.[6] Cu K-edge XAS spectra of side-on bound nitrosobenzene in formally Cu^{I} β-diketiminato complexes also reveals the redox non-innocence of nitrosobenzene.[7] Moreover, nitrosobenzene ligands in the formally zerovalent complexes $(ArNC)_2Pd(\kappa^1\text{-}N\text{-ONPh})_2$ and $(ArNC)_2Pd(\eta^2\text{-}O,N\text{-ONAr}')$ (Ar = 2,6-(2,6-$^{i}Pr_2C_6H_3$)$_2$C$_6$H$_3$ and Ar′ = 2-Me-C$_6$H$_4$ or 2-tol; Figure 1) are best described as $(PhNO)^{\bullet-}$ and $(2\text{-tol-NO})^{2-}$ ligands, respectively.[8]

A wide array of previously reported bimetallic *C*-nitroso complexes exhibit greater activation of the RN=O bond as compared to that exhibited by monometallic complexes (Figure 1).[2b,9] For instance, coordination of two β-diketiminato nickel(I) fragments to a nitrosoarene leads to $\{[Me_2NN]Ni\}_2(\mu\text{-}\eta^2\text{:}\eta^2\text{-ONAr})$ (Ar = 3,5-Me$_2$C$_6$H$_3$)[9a] with a N–O distance of 1.440(4) Å, considerably longer than in free aryl nitroso compounds (1.21–1.23 Å).[2b] A dinuclear copper complex $LCu(\mu\text{-}\eta^2\text{:}\eta^2\text{-ONAr})CuL$ (L = tetramethylpropylenediamine, Ar = 4-NO$_2$-C$_6$H$_4$) with a N–O distance of 1.457(9) Å has been recently reported to possess a similar electronic structure as found in dicopper-(μ-η^2:η^2-peroxo) species.[10] The electron-rich β-diketiminato Co^{I} complex $[Me_2NN]Co(\eta^6\text{-toluene})$ provides an extreme case of N–O bond activation, completely cleaving the ArN=O bond to give $\{[Me_2NN]Co\}_2(\mu\text{-O})(\mu\text{-NAr})$ (Ar = 3,5-Me$_2$C$_6$H$_3$).[9b]

Herein we report the successful isolation of an unusual mononuclear β-diketiminato $[Ni^{II}](\eta^2\text{-ONPh})^{\bullet-}$ complex that features a nitrosobenzene radical anion ligand. Interestingly, one-electron reduction of this $[Ni^{II}](\eta^2\text{-ONPh})^{\bullet-}$ species is ligand-centered and provides a $[Ni^{II}](\eta^2\text{-ONPh})^{2-}$ complex, which serves as a model of a doubly deprotonated hydroxylamine ligand. Furthermore, the redox transformations observed are reminiscent of those between bound superoxide[11] ($O_2^{\bullet-}$) and peroxide[12] (O_2^{2-}) ligands, which allows for direct comparison of reactivity patterns including H-atom abstraction by novel $[Ni^{II}](\eta^2\text{-ONPh})^{\bullet-}$ species.

The Ni^{I} "ate"-complex $\{[^{i}Pr_2NN_{F6}]Ni^{I}(\mu\text{-Br})\}Li(Et_2O)$(dme) (**2**) may be prepared in moderate yield by KC_8 reduction of complex $\{[^{i}Pr_2NN_{F6}]Ni^{II}(\mu\text{-Br})_2\}Li(THF)_2$ (**1**; Scheme 1 a). This d^9 Ni^{I} species **2** possesses a rhombic frozen-glass EPR spectrum ($g_1 = 2.439$, $g_2 = 2.127$, $g_3 = 2.105$; Supporting Information, Figure S2) similar to other three-

[*] Dr. S. Kundu, Dr. J. A. Bertke, Prof. Dr. T. H. Warren
Department of Chemistry, Georgetown University
Box 571227, Washington, DC 20057-1227 (USA)
E-mail: skundu.chem@gmail.com
thw@georgetown.edu
Prof. Dr. S. C. E. Stieber, Dr. M. G. Ferrier, Dr. S. A. Kozimor
Inorganic, Isotope and Actinide Chemistry
Los Alamos National Laboratory
Los Alamos, NM 87545 (USA)
Prof. Dr. S. C. E. Stieber
Department of Chemistry and Biochemistry
California State Polytechnic University
Pomona, CA 91768 (USA)
E-mail: sestieber@cpp.edu
Supporting information and the ORCID identification number(s) for the author(s) of this article can be found under http://dx.doi.org/10.1002/anie.201605026.

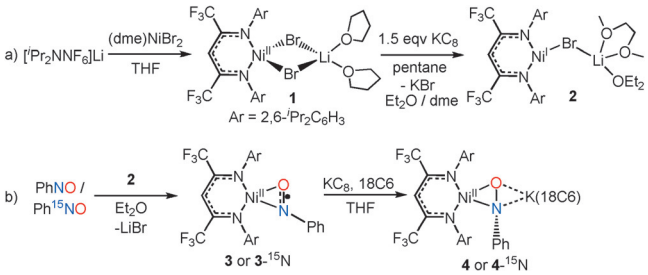

Scheme 1. a) Synthesis of [^{i}Pr$_2$NN$_{F6}$]Ni^{I} precursor **2**, b) Activation of nitrosobenzene to isolate [^{i}Pr$_2$NN$_{F6}$]Ni^{II}(η^2-ONPh)$^{\bullet/-}$ (**3**) and [^{i}Pr$_2$NN$_{F6}$]Ni^{II}(μ-η^2:η^2-ONPh)K[18C6] (**4**).

coordinate Ni^{I} β-diketiminato complexes.[13] Addition of one equiv PhNO to a solution of **2** in diethyl ether at room temperature results in an immediate color change from purple to orange. Crystallization from pentane provides the nitrosobenzene complex [^{i}Pr$_2$NN$_{F6}$]Ni(η^2-ONPh) (**3**) in 94% yield (Scheme 1b). X-ray diffraction analysis (Figure 2)

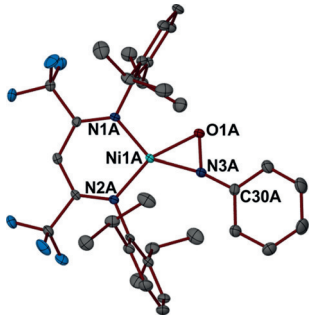

Figure 2. X-ray structure of one molecule of **3**; ellipsoids set at 50% probability.[24]

reveals the presence of two independent square planar β-diketiminato [Ni](η^2-ONPh) moieties in the asymmetric unit with the sum of angles around Ni of 359.98(6)° (molecule A) and 359.94(7)° (molecule B). This nitrosobenzene adduct **3** possesses short Ni–N$_{\beta\text{-dik}}$ distances (molecule A: 1.8511(15), 1.8525(14) Å; molecule B: 1.8544(15) Å, 1.8537(15) Å) along with short Ni–N and Ni–O bond distances to the nitrosobenzene ligand (molecule A: 1.8347(16) and 1.8744(13) Å; molecule B: 1.8329(17) and 1.8834(14) Å, respectively). The PhN–O distances in **3** (N3A–O1A, 1.3270(19) Å and N3B–O1B, 1.323(2) Å) are very close to those in previously reported mononuclear Cu complexes [Me$_2$NN]Cu(η^2-ONAr) (Ar = 3,5-Me$_2$C$_6$H$_3$, Ph) (1.333(4)–1.336(6) Å)[9a] but significantly shorter than in dinuclear {[Me$_2$NN]Ni}$_2$(μ-η^2:η^2-ONAr) (Ar = 3,5-Me$_2$C$_6$H$_3$; 1.440(4) Å).[9a] Importantly, the PhN–O distances in **3** are significantly longer than that in free monomeric *C*-nitroso compounds (1.21–1.23 Å),[2b] signaling a decrease in the N–O bond order. In contrast to [Cu](η^2-ONAr) complexes, however, the PhNO aromatic ring in [^{i}Pr$_2$NN$_{F6}$]Ni(η^2-ONPh) (**3**) is essentially in the plane of the Ni–O–N unit (deviations of 10.9° and 6.7°, respectively) allowing for possibility of extended π-conjugation into the nitrosobenzene aryl substituent.[14] Accordingly, the C30A–N3A and C30B–N3B bond distances of 1.370(2) and 1.372(2) Å in **3** are considerably shorter than corresponding C–N bond lengths of 1.438(6) and 1.442(6) Å in [Me$_2$NN]Cu(η^2-ONPh).[9a]

Spectral characterization of **3** indicates significant reduction of the nitrosobenzene ligand consistent with a (ONPh)$^{\bullet/-}$ formulation. The IR spectrum of **3** (Supporting Information, Figure S4) exhibits a ν_{NO} band at 968 cm^{-1} (950 cm^{-1} for **3**-^{15}N), dramatically lower than that of free PhNO (1506 cm^{-1}).[2b] Moreover, this stretching frequency is significantly lower than that found in [Me$_2$NN]Cu(η^2-ONAr) (1113 cm^{-1}), indicating greater reduction of the PhNO ligand by the monovalent [^{i}Pr$_2$NN$_{F6}$]Ni core. Isotropic X-band EPR spectra of **3** and **3**-^{15}N in THF at 293 K (Figure 3; Supporting Information, Figure S5) illustrate characteristic $S = {}^1/_2$ isotropic signals for a ligand-centered radical with strong coupling to a single $^{14/15}$N nucleus. Each gives a signal centered at $g_{iso} = 2.018$ consisting of three lines ($A_{iso}(^{14}N) =$ 39.1 MHz for **3**) or two lines ($A_{iso}(^{15}N) = 53.7$ MHz for **3**-^{15}N), respectively. Notably, the ratio of isotropic hyperfine coupling constants $A_{iso}(^{15}N)/A_{iso}(^{14}N) = 1.37$ is very close to the ratio of corresponding gyromagnetic ratios (1.40). Simulation of frozen-glass X-band EPR spectra of **3** and **3**-^{15}N in THF at 20 K (Supporting Information, Figure S5) reveals three closely spaced g values ($g_1 = 2.034$, $g_2 = 2.013$, $g_3 = 1.996$) with highly anisotropic coupling to the nitrosobenzene N nucleus ($A_3(^{14}N) = 81$ MHz for **3**; $A_3(^{15}N) = 114$ MHz for **3**-^{15}N). Notably, the narrow spread of g-values near the free electron value ($g_e = 2.0023$) suggests a ligand-centered radical.

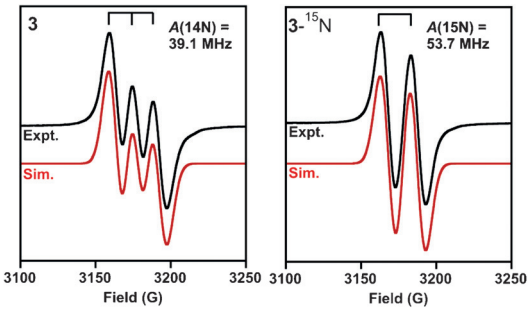

Figure 3. X-band EPR spectra (black trace) of **3** and **3**-^{15}N in tetrahydrofuran at 293 K. Frequency = 8.977388 GHz, power = 0.99 mW, Mod-Width = 0.35 mT. Simulations (red trace) provide $g_{iso} = 2.0183$ with $A_{iso}(^{14}N) = 39.1$ MHz and $A_{iso}(^{15}N) = 53.7$ MHz.

DFT calculations (B3LYP-TZVP/SV(P)) (Supporting Information, section S13) also predict that the unpaired electron resides mainly on the PhNO ligand of **3** (Figure 4c). The predicted spin density of 0.51 e$^-$ at N is consistent with the large hyperfine coupling to N observed by EPR. Moreover, an N–C bond shortening is also predicted for free PhNO$^{\bullet/-}$ (1.387 Å) as compared to the neutral PhNO (1.449 Å) by DFT. Thus, structural, spectroscopic, and DFT analyses point to **3** as a neutral $S_{total} = {}^1/_2$ complex with a low-spin β-diketiminato Ni^{II} center (d^8, $S_{Ni} = 0$) and a (η^2-ONPh)$^{\bullet/-}$ ligand ($S_{PhNO} = {}^1/_2$).

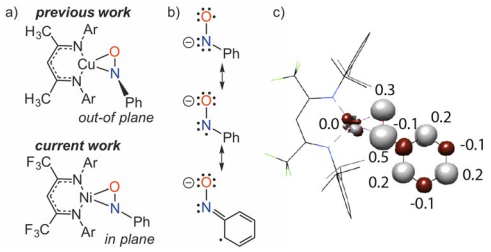

Figure 4. a) Out-of-plane[9a] and in-plane nitrosobenzene ligands bound to β-diketiminato-copper/nickel complexes. b) Resonance structures of nitrosobenzyl radical anion. c) Mulliken spin density plot for **3**. Spin density: gray = positive, brown = negative.

The cyclic voltammogram of **3** in THF at room temperature exhibits a reversible reduction wave centered at −890 mV vs. Cp_2Fe^+/Cp_2Fe (Supporting Information, Figure S6) that suggests the possibility of isolating the one-electron reduced form of **3**. Addition of a slight excess of potassium-graphite (KC_8) along with an equimolar amount of 18-crown-6 (18C6) in THF leads to a rapid color change from orange to dark violet. Crystallization of the product from diethyl ether/ pentane provides {[^{i}Pr$_2$NN$_{F6}$]Ni^{II}(μ-η^2:η^2-ONPh)}K[18C6] (**4**) in 91% yield (Figure 5). As in **3**, this

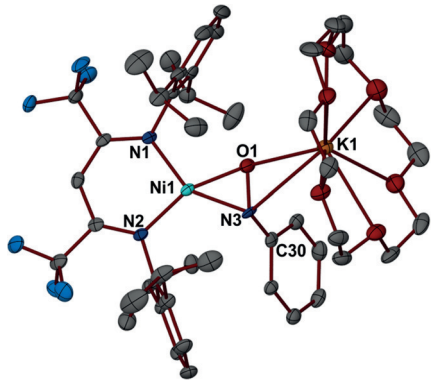

Figure 5. Molecular structure of **4**; ellipsoids set at 50% probability.[24]

reduced nitrosobenzene adduct **4** exhibits square-planar coordination about Ni with short Ni–N (1.878(3) –1.927-(2) Å) and Ni–O (1.851(2) Å) distances consistent with a low-spin Ni^{II} center. The O1–N3 bond distance of the nitrosobenzene moiety in **4** (1.382(3) Å) is longer than in **3** (1.327(2) and 1.323(2) Å) indicating further reduction of this ligand. Furthermore, the nitrosobenzene N3–C30 bond distance in **4** (1.406(4) Å) lengthens relative to **3** (1.370(2) and 1.372(2) Å) and the Ph group moves significantly out of the Ni-O-N plane (Ni-O1-N3-C30 torsion angle: 112.2°). The [18C6]K$^+$ cation in **4** is tightly coordinated to both the oxygen and nitrogen atoms of the reduced PhNO ligand with K1–O1 and K1–N1 distances of 2.716(2) and 3.082(3) Å, respectively.

Importantly, {[^{i}Pr$_2$NN$_{F6}$]Ni^{II}(μ-η^2:η^2-ONPh)}K[18C6] (**4**) is diamagnetic. The ^{1}H NMR spectrum of **4** in [D$_8$]THF (Supporting Information, Figure S8) shows resonances typical for diamagnetic β-diketiminato nickel complexes.[15] While the ^{15}N NMR spectrum of **4**-^{15}N exhibits a sharp singlet at 233.9 ppm (vs. liquid NH_3; Supporting Information, Figure S9), the ^{19}F NMR spectrum (Supporting Information, Figure S10) depicts two inequivalent backbone CF_3 groups at $\delta = -61.7$ and −62.6 ppm, consistent with static binding of the η^2-ONPh moiety. Hence, these multinuclear NMR studies (Supporting Information, Figures S8–S10) together with the square-planar geometry of the Ni center indicate that **4** is best described as an anionic $S_{total} = 0$ complex comprising of a low-spin [Ni^{II}] center (d^8, $S_{Ni} = 0$) bound to a (PhNO)$^{2-}$ ligand ($S_{PhNO} = 0$). Consistent with this formulation, the IR spectrum of anionic **4** and **4**-^{15}N show ν_{NO} vibrational bands at 765 and 751 cm^{-1} (Supporting Information, Figure S11), indicating significant further reduction of the nitrosobenzene ligand as compared to neutral **3** and **3**-^{15}N (968 and 950 cm^{-1}).

Ni K-edge X-ray absorption spectroscopy (XAS) was used to probe the nickel oxidation state in reduced nitrosobenzene adducts **3** and **4**. The pre-edge energy in Ni K-edge XAS is associated with Ni_{1s}-to-Ni_{3d} transitions and typically shifts 1 eV per one-electron redox event at Ni.[16] Figure 6 compares

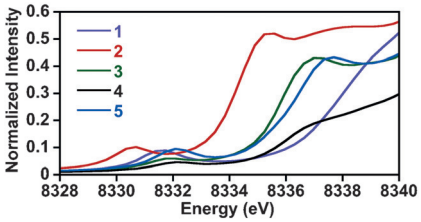

Figure 6. Normalized Ni K-edge pre-edge features of **1**–**5** obtained from X-ray absorption spectroscopy (XAS) at 77 K. Figure S26 depicts the full Ni K-edge XAS spectra.

the Ni K-edge spectra of **3** and **4** with reference complexes **1**, **2**, and **5**. The pre-edge feature at 8330.6 eV for the Ni^{I} complex **2** shifts to 8331.6 eV for the Ni^{II} complex **1**. The pre-edge energies for nitrosobenzene adducts **3** (at 8331.9-(1) eV) and **4** (8332.0(1) eV), however, are similar to the bonafide [Ni^{II}] complexes **1** and **5** (8332.0(1) eV), supporting Ni^{II} centers in both **3** and **4**. The rising edge feature (8334–8338 eV) is a Ni_{1s}-to-Ni_{4p} shakedown transition that is sensitive to geometry at Ni. As previously observed,[16] this feature is absent for the tetrahedral complex **1**, but present for all square-planar complexes **2**–**5**. These XAS results further validate the description of the neutral nitrosobenzene adduct **3** as [Ni^{II}](η^2-ONPh)$^{\bullet/-}$ that undergoes nitrosobenzene reduction to give the (η^2-ONPh)$^{2-}$ ligand bound to a [Ni^{II}] center in anionic **4**. TDDFT calculations are consistent with the experimental data (Supporting Information, Section S13).

We then examined the reactivity patterns of nitrosbenzene adducts **3** and **4** possessing (η^2-ONPh)$^{\bullet/-}$ and (η^2-ONPh)$^{2-}$ ligands, respectively. Reaction of **3** with $NO_{(g)}$ conceptually illustrates radical coupling between the *N*-centered spins of the (η^2-ONPh)$^{\bullet/-}$ ligand in **3** and free NO (Scheme 2). Reaction of **3** with 1 equiv $NO_{(g)}$ in diethyl ether at room temperature leads to immediate generation of the diamagnetic [Ni^{II}]-diazeniumdiolate complex **5** in near quantitative yield (Scheme 2a). X-ray diffraction analysis (Scheme 2b) reveals κ^2-O,O′-coordination of a nearly planar

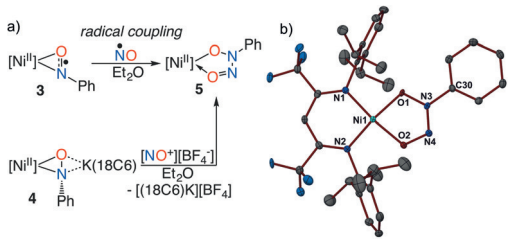

Scheme 2. a) Conversion of **3** and **4** into **5**. b) Molecular structure of **5**; ellipsoids set at 50% probability.[24]

$(O_2N_2Ph)^{1-}$ ligand to the β-diketiminato Ni^{II} center, similar in form to related $[Ni^{II}](\kappa^2\text{-}O_2N_2Ar)$ complexes formed by addition of NO to β-diketiminato $[Ni]_2(\mu\text{-}\eta^2\text{:}\eta^2\text{-}OAr)$ species[9a] or ONAr addition to [Ni]–NO complexes.[17] On the other hand, the reduced anionic **4** possessing a $(\eta^2\text{-}ONPh)^{2-}$ ligand cleanly reacts with $[NO^+]BF_4^-$ at room temperature to give the $[Ni^{II}](\kappa^2\text{-}O_2N_2Ph)$ complex **5** in 87% yield.

Given their isoelectronic nature, we anticipated that the $(ONPh)^{\bullet/-}/(ONPh)^{2-}$ redox couple might exhibit reactivity patterns demonstrated by the more familiar superoxo $(O_2)^{\bullet/-}$/ peroxo $(O_2)^{2-}$ species. For instance, mononuclear superoxo complexes $[M](O_2^-)$ have been implicated in H-atom abstraction (HAA) reactions to give reactive hydroperoxo species [M]–OOH that are difficult to isolate and characterize.[18] In contrast, reduced peroxo species $[M](O_2^{2-})$ can afford such [M]–OOH species via protonation.[19] Recent reports of β-diketiminato $[Ni^{II}](\eta^2\text{-superoxo})$[11] and $\{[Ni^{II}](\mu\text{-}\eta^2\text{:}\eta^2\text{-peroxo})\}K$[12] complexes isostructural to **3** and **4**, respectively, bring these challenges into focus. For instance, a transient [Ni^{II}]–OOH species was proposed during the hydrogen atom abstraction (HAA) of a substituted phenol by a $[Ni^{II}](\eta^2\text{-superoxo})$ complex from the O–H bond of substituted phenol.[20]

Superoxo analogue **3** possessing a radical anion nitrosobenzene ligand $(\eta^2\text{-}ONPh)^{\bullet-}$ bound to a [Ni^{II}] center undergoes clean HAA reactivity with 1,4-cyclohexadiene (C–H BDE = 76 kcal mol^{-1})[21] at 65 °C (Scheme 3a) to give the diamagnetic Ni^{II} nitroxide $[^iPr_2NN_{F6}]Ni(\eta^2\text{-}ONHPh)$ (**6**) in 88% yield. DFT studies indicate that single HAA of 1,4-cyclohexadiene by **3** to form **6** is uphill with $\Delta G = +10.9$ kcal mol^{-1}. The X-ray structure of **6** (Scheme 3b) reveals its square-planar geometry featuring an η^2-ONHPh nitroxide ligand with short Ni–N3 and N–O distances of 1.9153(10) and

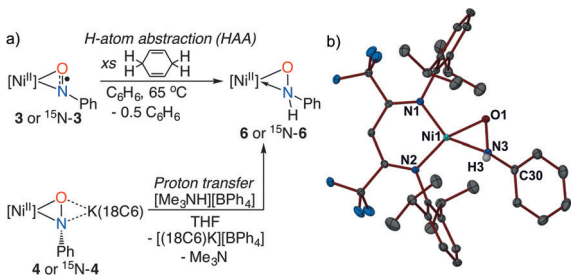

Scheme 3. a) Conversion of **3** and **4** to **6** via hydrogen atom abstraction (HAA) and proton transfer routes, respectively. b) Molecular structure of **6**; ellipsoids set at 50% probability.[24]

1.8381(9) Å. The nitroxide N–O distance of 1.3829(12) Å in **6** is nearly identical to the N–O distance in reduced **4** (1.382-(3) Å). The ^{1}H NMR spectrum of **6** possesses a singlet for the N–H moiety at $\delta = 5.16$ ppm which splits into a doublet with $^1J_{NH} = 85.7$ Hz in the ^{15}N-labeled sample **6**-^{15}N (Supporting Information, Figures S16–S19). This nitroxide complex **6** may also be prepared in 91% yield by protonation of the anionic $(\eta^2\text{-}ONPh)^{2-}$ complex **4** with one equiv $[Me_3NH][BPh_4]$ (Scheme 3a).

These findings illustrate the redox non-innocence of nitrosobenzene through a family of reduced species bound to a common β-diketiminato nickel(II) fragment. Key structural and spectroscopic changes accompany interconversion between the one-electron redox couple of bound $(\eta^2\text{-}ONPh)^{\bullet/-}/(\eta^2\text{-}ONPh)^{2-}$ ligands that are related to more familiar superoxo $(O_2)^{\bullet/-}$/ peroxo $(O_2)^{2-}$ species (Scheme 4), although

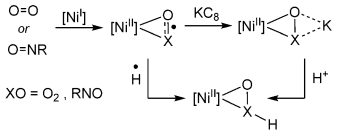

Scheme 4. Similarity between oxygen and *C*-nitroso ligand-based reactivity. active forms of *C*-nitroso ligands.

free PhNO and O_2 possess different ground electronic states. Importantly, the one-electron radical anion $(\eta^2\text{-}ONPh)^{\bullet/-}$ ligand in $[^iPr_2NN_{F6}]Ni(\eta^2\text{-}ONPh)$ (**3**) serves as a competent H-atom abstracting reagent, affording the stable nitroxide complex $[^iPr_2NN_{F6}]Ni(\eta^2\text{-}ONHPh)$ (**6**) upon reaction with 1,4-cyclohexadiene. The present study not only offers a lens to view HAA reactivity of metal–superoxide complexes suggested in the reaction of metal complexes with dioxygen,[22] but also anticipates the possibility of redox non-innocence in the study of related metal nitroxyl [M](HNO) complexes.[23]

Acknowledgements

T.H.W. acknowledges funding from the National Science Foundation (CHE-1459090 and CHE-1337975) and the Georgetown Environment Initiative. S.A.K. acknowledges the Heavy Element Chemistry Program by the Division of Chemical Sciences, Geosciences, and Biosciences, Office of Basic Energy Sciences (BES), U.S. Department of Energy (DOE), and Seaborg Institute Postdoctoral Fellowship (S.C.E.S., M.G.F.). LANL is operated by Los Alamos National Security, LLC, for the National Nuclear Security Administration of U.S. DOE (DE-AC52-06NA25396). Use of Stanford Synchrotron Radiation Lightsource, SLAC National Accelerator Laboratory, supported by DOE, Office of Science, BES (DE-AC02-76SF00515). S.C.E.S. acknowledges CPP College of Science and NSF XSEDE (CHE-150060, ACI-1053575).

Keywords: nickel · nitric oxide · nitrosobenzene · redox-active ligands · X-ray spectroscopy

How to cite: *Angew. Chem. Int. Ed.* **2016**, *55*, 10321 – 10325
Angew. Chem. **2016**, *128*, 10477 – 10481

[1] W. Flores-Santana, D. J. Salmon, S. Donzelli, C. H. Switzer, D. Basudhar, L. Ridnour, R. Cheng, S. A. Glynn, N. Paolocci, J. M. Fukuto, et al., *Antioxid. Redox Signal.* **2011**, *14*, 1659.
[2] a) P. Zuman, B. Shah, *Chem. Rev.* **1994**, *94*, 1621; b) J. Lee, L. Chen, A. H. West, G. B. Richter-Addo, *Chem. Rev.* **2002**, *102*, 1019.
[3] a) F. Doctorovich, D. E. Bikiel, J. Pellegrino, S. A. Suárez, M. A. Martí, *Acc. Chem. Res.* **2014**, *47*, 2907; b) F. Doctorovich, D. E. Bikiel, J. Pellegrino, S. A. Suárez, M. A. Martí, *Prog. Inorg. Chem.* **2014**, *58*, 145.
[4] M. R. Kumar, A. Zapata, A. J. Ramirez, S. K. Bowen, W. A. Francisco, P. J. Farmer, *Proc. Natl. Acad. Sci. USA* **2011**, *108*, 18926.
[5] a) S. E. I. Otsuka, *Inorg. Chem.* **1976**, *15*, 656; b) R. S. Srivastava, M. A. Khan, K. M. Nicholas, *J. Am. Chem. Soc.* **2005**, *127*, 7278; c) R. S. Srivastava, N. R. Tarver, K. M. Nicholas, *J. Am. Chem. Soc.* **2007**, *129*, 15250.
[6] M. S. Askari, B. Girard, M. Murugesu, X. Ottenwaelder, *Chem. Commun.* **2011**, *47*, 8055.
[7] a) N. C. Tomson, K. D. Williams, X. Dai, S. Sproules, S. DeBeer, T. H. Warren, K. Wieghardt, *Chem. Sci.* **2015**, *6*, 2474; b) K. D. Williams, A. J. P. Cardenas, J. D. Oliva, T. H. Warren, *Eur. J. Inorg. Chem.* **2013**, 3812.
[8] N. C. Tomson, L. A. Labios, T. Weyhermüller, J. S. Figueroa, K. Wieghardt, *Inorg. Chem.* **2011**, *50*, 5763.
[9] a) S. Wiese, P. Kapoor, K. D. Williams, T. H. Warren, *J. Am. Chem. Soc.* **2009**, *131*, 18105; b) X. Dai, P. Kapoor, T. H. Warren, *J. Am. Chem. Soc.* **2004**, *126*, 4798.
[10] M. S. Askari, M. Orio, X. Ottenwaelder, *Chem. Commun.* **2015**, *51*, 11206.
[11] S. Yao, E. Bill, C. Milsmann, K. Wieghardt, M. Driess, *Angew. Chem. Int. Ed.* **2008**, *47*, 7110; *Angew. Chem.* **2008**, *120*, 7218.
[12] S. Yao, Y. Xiong, M. Vogt, H. Grützmacher, C. Herwig, C. Limberg, M. Driess, *Angew. Chem. Int. Ed.* **2009**, *48*, 8107; *Angew. Chem.* **2009**, *121*, 8251.
[13] a) G. Bai, P. Wei, D. W. Stephan, *Organometallics* **2005**, *24*, 5901; b) N. A. Eckert, A. Dinescu, T. R. Cundari, P. L. Holland, *Inorg. Chem.* **2005**, *44*, 7702; c) E. Kogut, H. L. Weincko, L. Zhang, D. E. Cordeau, T. H. Warren, *J. Am. Chem. Soc.* **2005**, *127*, 11248; d) S. Pfirrmann, S. Yao, B. Ziemer, R. Stösser, M. Driess, C. Limberg, *Organometallics* **2009**, *28*, 6855.
[14] A similar coplanar orientation of the phenyl ring and M-N-O plane allowed extended delocalization of the unpaired electron throughout the nitrosobenzyl radical anion in structurally characterized $[M](PhNO)^{\bullet-}$ complexes (M = Cu, Pd; see Refs. [6] and [8]).
[15] C. Köthe, R. Metzinger, C. Herwig, C. Limberg, *Inorg. Chem.* **2012**, *51*, 9740.
[16] a) G. J. Colpas, M. J. Maroney, C. Bagyinka, M. Kumar, W. S. Willis, S. L. Suib, N. Baidya, P. K. Maascharak, *Inorg. Chem.* **1991**, *30*, 920; b) M. Kawai, T. Yamaguchi, S. Masaoka, F. Tani, T. Kohzuma, L. Chiang, T. Storr, K. Mieda, T. Ogura, R. K. Szilagyi, Y. Shimazaki, *Inorg. Chem.* **2014**, *53*, 10195; c) F. Heims, F. F. Pfaff, S.-L. Abram, E. R. Farquhar, M. Bruschi, C. Greco, K. Ray, *J. Am. Chem. Soc.* **2014**, *136*, 582; d) S. A. Yao, V. Martin-Diaconescu, I. Infante, K. M. Lancaster, A. W. Götz, S. DeBeer, J. F. Berry, *J. Am. Chem. Soc.* **2015**, *137*, 4993.
[17] S. C. Puiu, T. H. Warren, *Organometallics* **2003**, *22*, 3974.
[18] Y.-M. Lee, S. Hong, Y. Morimoto, W. Shin, S. Fukuzumi, W. Nam, *J. Am. Chem. Soc.* **2010**, *132*, 10668.
[19] F. Li, K. K. Meier, M. A. Cranswick, M. Chakrabarti, K. M. Van Heuvelen, M. Eckard, L. Que, *J. Am. Chem. Soc.* **2011**, *133*, 7256.
[20] A. Company, S. Yao, K. Ray, M. Driess, *Chem. Eur. J.* **2010**, *16*, 9669.
[21] Y.-R. Luo, *Comprehensive handbook of chemical bond energies*, Taylor & Francis, New York, **2007**.
[22] a) J. Cho, J. Woo, W. Nam, *J. Am. Chem. Soc.* **2010**, *132*, 5958; b) K. Ray, F. F. Pfaff, B. Wang, W. Nam, *J. Am. Chem. Soc.* **2014**, *136*, 13942; c) W. Nam, *Acc. Chem. Res.* **2015**, *48*, 2415.
[23] a) R. Melenkivitz, J. S. Southern, G. L. Hillhouse, T. E. Concolino, L. M. Liable-Sands, A. L. Rheingold, *J. Am. Chem. Soc.* **2002**, *124*, 12068; b) P. J. Farmer, F. Sulc, *J. Inorg. Biochem.* **2005**, *99*, 166; c) E. G. Abucayon, R. L. Khade, D. R. Powell, Y. Zhang, G. B. Richter-Addo, *J. Am. Chem. Soc.* **2016**, *138*, 104.
[24] CCDC 1456603 – 1456608 (**1** – **6**) contain the supplementary crystallographic data for this paper. These data are provided free of charge by The Cambridge Crystallographic Data Centre. See also the Supporting Information, Section S11.

Received: May 23, 2016
Published online: July 29, 2016

